Journal of Power Sources 240 (2013) 753–758

Contents lists available at SciVerse ScienceDirect

Journal of Power Sources

journal homepage: www.elsevier.com/locate/jpowsour

Tri-functional Nb_2O_5 nano-islands coated on an indium tin oxide layer for a highly efficient dye-sensitized plastic photoanode

Saori Morita [a], Tzu-Chien Wei [a,b,*], Masashi Ikegami [a], Tsutomu Miyasaka [a]

[a] Graduate School of Engineering, Toin University of Yokohama, Japan
[b] Department of Chemical Engineering, National Tsing-Hua University, Taiwan

HIGHLIGHTS

- We coated Nb_2O_5 nano-islands on plastic substrate via a low-temperature process.
- We proposed there are three functions of this coating.
- Conversion efficiency improved from 5.19% to 5.81% is achieved.

GRAPHICAL ABSTRACT

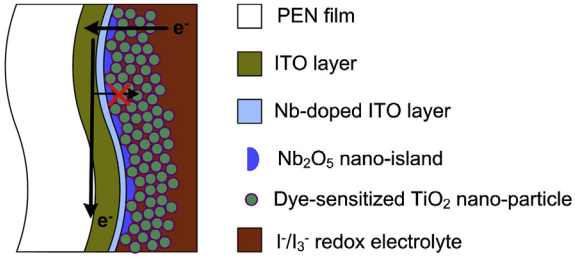

ARTICLE INFO

Article history:
Received 26 December 2012
Received in revised form
7 May 2013
Accepted 14 May 2013
Available online 28 May 2013

Keywords:
Plastic
Low temperature
Interfacial recombination
Adhesion

ABSTRACT

Tri-functional Nb_2O_5 nano-islands are deposited on indium tin oxide (ITO) transparent conductive layer on a plastic sheet (ITO PEN) as the anode substrate for a dye-sensitized solar cell by spin-coating a niobium precursor solution and heating at 150 °C for 10 min. The films are characterized by means of time of flight secondary ion mass spectrometry (TOF/SIMS), field emission scanning electron microscopy (FESEM), atomic force microscopy (AFM), small angle X-ray diffraction (SAXRD), electrochemical impedance spectroscopy (EIS), four-probe meter and current–voltage curves. It was found that the Nb_2O_5 coating exhibits at least three functions, including suppressing interfacial recombination, improving TiO_2 film adhesion and lowering sheet resistance of the ITO PEN film; these functions are all beneficial to photovoltaic performance in a dye-sensitized solar cell. Finally, a plastic dye-sensitized solar cell with this Nb_2O_5-treated photoanode was fabricated, and a remarkable improvement of power conversion efficiency (PCE), from 5.19% to 5.81% was demonstrated.

1. Introduction

The dye-sensitized solar cell (DSSC) is a promising device for inexpensive, large-scale use of solar electricity, due to its low material and equipment cost and high power conversion efficiency (PCE) [1–5]. In particular, fabricating a DSSC on a flexible substrate, such as plastic films or metal sheets, is even more attractive due to its light weight and the potential of roll-to-roll, large volume production. At the core of a DSSC is a dye-sensitized photoanode. In general, a flexible photoanode is comprised of a sensitizing TiO_2 film on a transparent conductive plastic film, such as indium-coped tin oxide on polyethylene naphthalate (ITO PEN). This allows back illumination on the counter-electrode side during operation resulting in higher incident light utilization than a front illuminated device, which is commonly found when sensitized TiO_2 film is prepared on metal sheet or metal plate [6,7]. However, when a plastic film is used as the substrate, all the processing temperatures must be below the glass transition temperature of the plastic. Several methods, such as electrophoresis deposition [8,9], chemical

* Corresponding author. No.101, Section 2, Kuang-Fu Road, Hsinchu 30013, Taiwan. Fax: +886 35715131x33669.
E-mail addresses: tcwei@mx.nthu.edu.tw, hibinowei@hotmail.com (T.-C. Wei).

0378-7753/$ – see front matter © 2013 Elsevier B.V. All rights reserved.
http://dx.doi.org/10.1016/j.jpowsour.2013.05.053

sintering [10], mechanical pressing [11–13], and others have been proposed to reach this goal via a low-temperature process. These methods were found to be capable of interconnecting the TiO_2 nano-particles of the coating film, which is crucial for efficient electron transportation in a DSSC.

It has been proved that charge transport from substrate to oxidized species (usually tri-iodide) in the electrolyte is one of the major charge loss routes in a DSSC [14–16]. To minimize this loss, a compact and thin metal oxide layer is coated on the substrate to prevent the photo-electrons from direct contact with the tri-iodides [15–20]. Of the various metal oxide coatings, niobium oxide (Nb_2O_5) has shown a conduction band (CB) which is approximately 100 mV higher than that of TiO_2 [19], while the effect of an Nb_2O_5 coating on fluorine-doped tin oxide (FTO) glass in suppressing interfacial charge recombination has been studied by Yanagida et al. [19,20]. However in their research, the Nb_2O_5 layer was coated on the rigid substrate either by vacuum sputtering [19] or spray pyrolysis, followed by a 500 °C post-heat treatment [20]. The former is highly energy consumptive, while the latter obviously cannot be used on plastic substrates. Therefore, there is a lack of studies on how to prepare a compact layer on a plastic substrate.

In addition, the surface of FTO glass is usually roughened to enhance optical utilization, while the surface of the ITO-derivative substrate is relatively smooth. Consequently, the physical adhesion between ITO and TiO_2 film is questionable, particularly in the case of bendable substrates like ITO PEN. In practice, poor adhesion results in local interfacial delamination, which often causes additional resistance and lowers the photovoltaic performance.

In this paper, the technical difficulties associated with the plastic photoanode described above were resolved by a singular Nb_2O_5 coating applied to an ITO PEN film by a low temperature and scalable process. This coating was found to suppress interfacial recombination between the substrate and the dye/TiO_2 layer, creating a rough surface to improve contact between the substrate and the dye/TiO_2 film. Surprisingly, it also decreased the sheet resistance of ITO PEN. Combining all these improvements, the PCE of DSSC with a plastic photoanode increased from between 5.19% to 5.81%.

2. Experimental

2.1. Preparation of niobium oxide coating

The Nb_2O_5 coating was prepared by spin-coating (1H-D7, Mikasa Co.) a precursor solution containing 0.5 mM niobium ethoxide in ethanol on the ITO PEN (15 Ω/sq, PECCELL Technologies) at 3000 rpm for 15 s. After preliminary drying in the air for 5 min, the coated plastic sheet was heated on a programmable hotplate at 150 °C for 10 min to complete the process.

2.2. Preparation of plastic TiO_2 photoanode and DSC fabrication

Before making the TiO_2 mesoporous film on a plastic substrate, a binder-free TiO_2 paste was first prepared as described previously [21,22]. The paste was then coated onto an Nb-treated ITO PEN film by the doctor-blade technique and dried at room temperature for 30 min. This was followed by heat treatment under air at 150 °C for 10 min to form a 5 μm-thick, mesoporous TiO_2 layer. Dye impregnation was made by immersing a plastic photoanode in a dye solution containing 0.3 mM N719 (Solaronix) in acetonitrile: t-butyl alcohol: ethanol (AN:tBA:EtOH = 2:1:1 in volume ratio) for 3 h at 40 °C. The DSSC was assembled by sandwiching the plastic photoanode and the counter electrode (platinum-sputtered FTO glass) with a hot-melt film (Surlyn, 25 μm) as the spacer. An electrolyte solution containing 0.02 M iodine (I_2), 0.4 M lithium iodide (LiI), 0.4 M tetrabutylammonium iodide (TBAI) and 0.1 M N-methylbenzimidazole iodide (NMBI) was then injected into the DSSC via a small hole drilled in the counter electrode.

2.3. Sample characterization

Field emission scanning electron microscopy (FESEM, Leo 1530 Gemini, German), atomic force microscopy (AFM, XE-70 Park system, Korea), small angle X-ray diffraction (SAXRD, Bruker, D8 Discover, USA) and time of flight secondary ion mass spectrometry (TOF/SIMS, PHI, TRIFT V nanoTOF, USA) were used to examine the morphology and structure of this Nb_2O_5-coated ITO PEN film. The current–voltage (*IV*) curve of the DSSC was recorded by a computer-controlled digital source meter (Keithley 2400, USA) under exposure of a standard solar simulator (PEC L12, Peccell, 1 Sun, AM1.5).

The electrochemical impedance spectroscopy (EIS) was recorded by scanning the DSSC with a computer-controlled potentialstat (VSP, Princeton Applied Research) from 200 kHz to 0.1 Hz with 10 mV amplitude at open circuit condition under 1 sun irradiation.

3. Results and discussion

3.1. Morphology of niobium oxide coating

The FESEM topographies of blank ITO PEN and Nb-coated ITO PEN are shown in Fig. 1(a) and (b), respectively. From Fig. 1(a), it can be seen that a large amount of round shaped, amorphous ITO is dispersed uniformly on the PEN substrate. It can also be observed that there are only a small number of rice-like ITO grains of ca. 100 nm in size randomly dispersed, indicating the absence of post-heat treatment after ITO sputtering. After the niobium species was coated on the ITO PEN (Fig. 1(b)), non-continuous, island-like

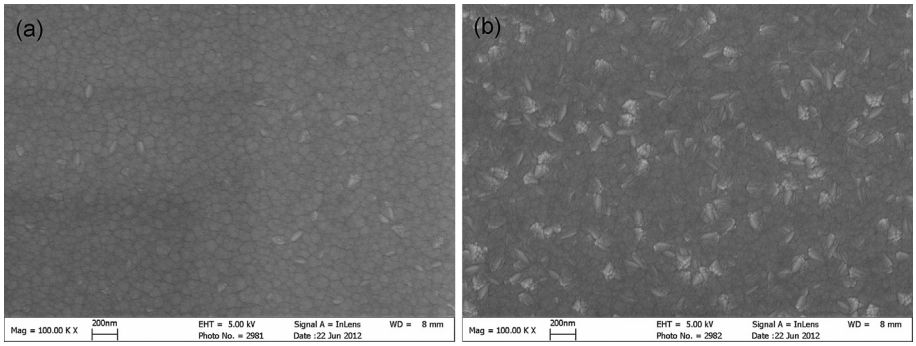

Fig. 1. Topographical FESEM images of (a) bare ITO PEN, showing a large portion of rounded, amorphous ITO grains with a few rice-like crystalline ITO grains, and (b) nano-islands of niobium species dispersed on the ITO substrate.

niobium grains sized from 100 to 200 nm can be seen dispersed on the ITO film. It was also found that the bottom ITO can still been seen from the topographical image, indicating that the niobium oxide formed there in a concentrated fashion during the post-heat treatment at 150 °C. In order to investigate the surface roughness of the Nb_2O_5-coated ITO PEN, the AFM topographies as well as three dimensional views were examined. From Fig. 2(a) and (b), it can be seen that the surface roughness of the blank ITO PEN is about 4 nm. After Nb_2O_5 was coated and heat-treated on the ITO PEN the surface became rougher by a factor of about 3 (12 nm), as can be found in Fig. 2(c) and (d). The increase of surface roughness was clearly a result of the Nb_2O_5 deposits as the nano-islands spread on the ITO ground. These nano-islands create more rugged surfaces than bare ITO film and are expected to improve the adhesion between substrate and dye-sensitized TiO_2 film. To further investigate the crystalline structure of the ultra-thin deposited Nb_2O_5 coating, SAXRD was performed on blank and Nb_2O_5-coated ITO PEN. It can be seen in Fig. 3 that the Nb_2O_5 peak (23.6 degree of 2 theta) overlapping the alpha form crystal of PEN substrate was detected on that sample with and Nb_2O_5 coating, while only the PEN signals (15.6, 23.6, 26.7, 33.4 degree of 2 theta) were detected in the blank ITO PEN. This indicates that Nb_2O_5 nano-islands are able to crystallize, even when the temperature of post-heating is only 150 °C.

The depth profile of Nb_2O_5-treated ITO PEN was examined by TOF/SIMS and is shown in Fig. 4; five elements including indium, tin, niobium, carbon and oxygen were analyzed. Among those elements, indium, tin and oxygen are the main elements for the ITO film, while niobium and carbon are ingredients of the niobium ethoxide precursor. Theoretically, the niobium signal should decrease sharply once the signals of tin and indium are detected, because the niobium coating should exist in the surface layer only.

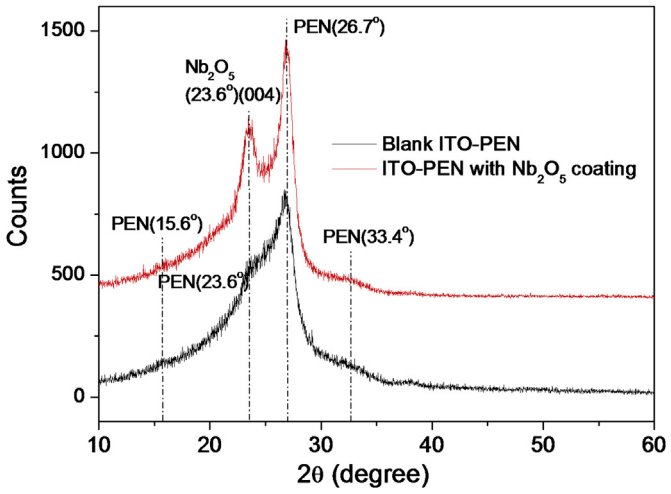

Fig. 3. SAXRD patterns of (a) bare ITO PEN, showing only the SnO_2 (110) peak at 26.7°, and (b) Nb-coated ITO PEN with an additional Nb_2O_5 (004) peak detected at 23.6°, confirming the existence of Nb_2O_5.

However, the niobium signal lasts until the etching depth reaches 35 nm, indicating that the niobium diffused into the ITO film during the heat treatment. Moreover, the decreasing pattern of niobium and carbon counts versus etching depth is not sharp, but moderate, implying that surface niobium and carbon species formed as a diffusion layer between the ITO and Nb_2O_5. Nb-doped ITO film has previously been found to have lower sheet resistance than undoped film, due to the distortion of lattice in the oxygen vacancies

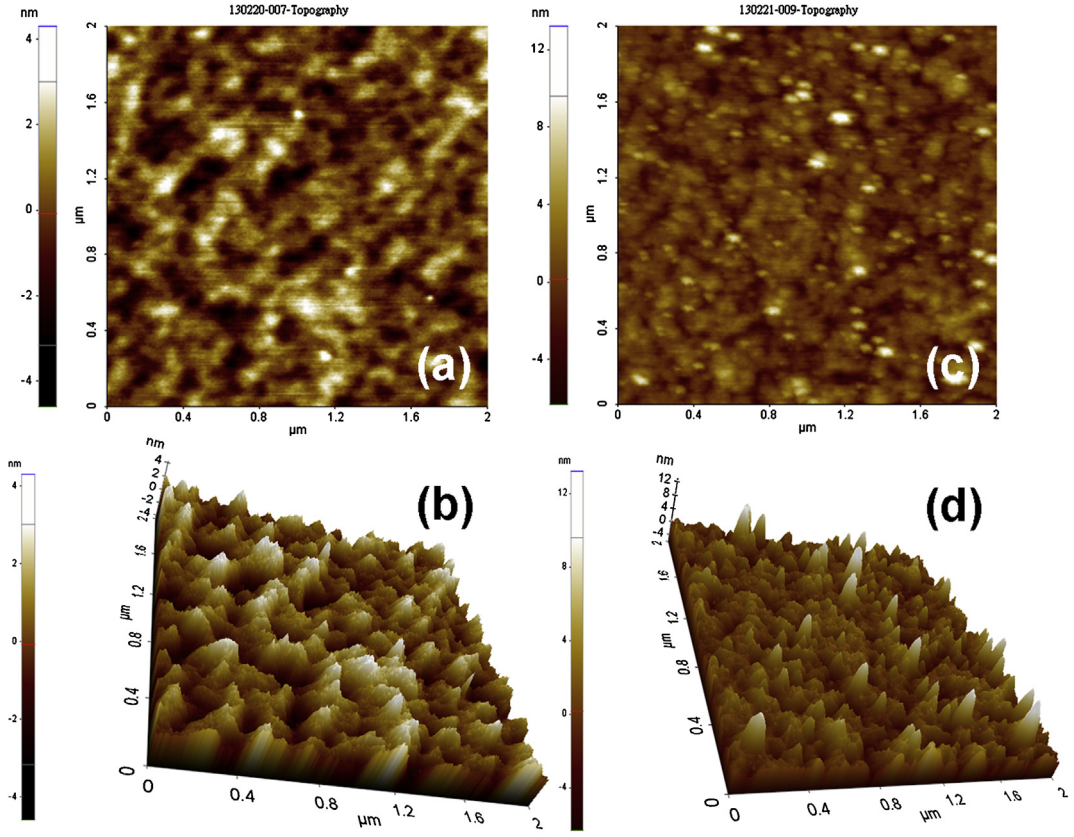

Fig. 2. AFM images of (a) topography, (b) 3D views of blank ITO PEN film and (c) topography, and (d) 3D views of Nb_2O_5-coated ITO PEN.

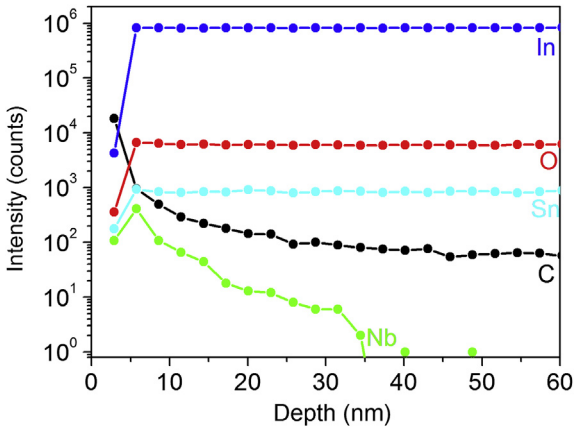

Fig. 4. TOF/SIMS evaluation recorded for Nb_2O_5 nano-islands coated ITO PEN.

[23]. To further prove this finding, the sheet resistance of Nb_2O_5-coated ITO PEN was examined by a 4 point probe station (Astellatech, SR4-A), and it was found that the sheet resistance decreased from 12.80 Ω/sq to 12.18 Ω/sq, which is consistent with the literature.

3.2. Effects of niobium oxide coating on an ITO PEN substrate

Suppression of interfacial recombination via the substrate was examined by scanning the *IV* curve of a 2-electrode testing cell composed of an ITO PEN with or without Nb_2O_5 coating (no dye/TiO_2 film) as the negative terminal, and plantized FTO glass as the positive terminal under darkness, as shown in Fig. 5 [14,24]. It can be observed from this Figure that under forward bias, the onset voltage of the *IV* curve, which represents the trigger point of charge transfer reaction from substrate to electrolyte, shifts by about 100 mV positively after Nb_2O_5 coating; this result is attributed to the fact that the CB of Nb_2O_5 is higher than that of FTO, so the reverse charge transport from FTO to TiO_2/dye film is energetically unfavorable. The possible electron transfer routes is cartooned on Fig. 6, showing the interfacial charge transport reaction has been suppressed by the Nb_2O_5 treatment.

The *IV* curves and their corresponding *IV* parameters of the DSSCs, composed of photoanode with and without Nb_2O_5 coating, are illustrated in Fig. 7. The PCE of a DSSC was calculated as:

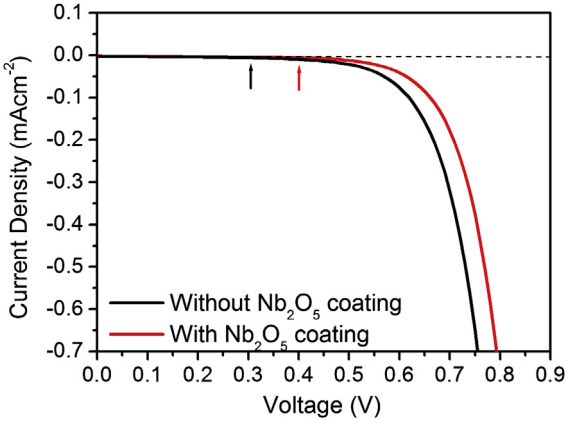

Fig. 5. Dark *IV* curves of the 2-electrode testing cells composed of an ITO PEN with and without Nb_2O_5 coating (no dye/TiO_2 film) as the negative terminal and platinized FTO glass as the positive terminal.

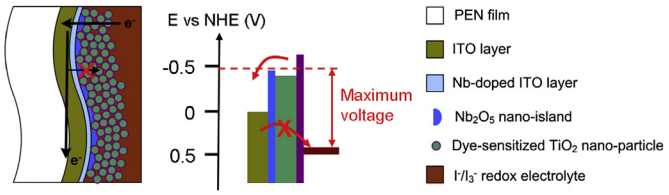

Fig. 6. Schematic view of interfaces in the Nb_2O_5-coated photoanode on ITO PEN and its imaginary electron transfer routes.

$$\text{PCE}\ (\%) = V_{OC} \times I_{SC} \times \text{FF}$$

where V_{OC} is the open circuit voltage, I_{SC} is the short circuit current density and FF is the fill factor. Clearly, V_{OC}, I_{SC} and FF are all important for a high efficiency DSSC. It can be seen from Fig. 5 that the most significant change in the curves is that the I_{SC} has increased from 11.17 to 11.78 mA cm^{-2}. Meanwhile, the FF is also improved from 0.65 to 0.69 and the V_{OC} is increased slightly from 0.71 V to 0.72 V. As a result, the PCE is improved from 5.19% to 5.81%. The suppression of interfacial recombination by introducing Nb_2O_5 coating onto the ITO PEN film is found to reduce charge loss at the ITO PEN/TIO_2 interface, and therefore is responsible for the increase of I_{SC} and V_{OC} [25]. However, it is worth noting that although suppression of recombination on the substrate of a well-assembled DSSC has been found to improve its performance, the improvement on a PCE should be minor because the increase on ISC is always accompanied by the decrease of FF in a DSSC that has had a robust assembly process. In our study, however, all of these three parameters affecting PCE (V_{OC}, I_{SC} and FF) increased. Therefore it is reasonable to speculate that there are one or more other factors affecting the *IV* behavior, other than the Nb_2O_5 coating.

To find out the other factor(s), the EIS was measured to investigate the interfacial behavior of the DSSCs. Fig. 8 presents the Nyquist plot of the DSSC made of plastic photoanode with or without Nb_2O_5 coating. It can be seen that the most significant change in EIS after Nb_2O_5 coating is that the arcs in both the high and middle frequencies have shrunk. Meanwhile the intercept of the real part of impedance (Z') in the highest frequency region also decreases. An equivalent circuit fitting our measuring conditions (high light intensity at open circuit) has been presented by Fabregat-Santiago et al. [26–28] and is illustrated in Fig. 9. In this simplified transmission line model, the key impedance elements are: series resistance (R_S), representing the sheet resistance of the ITO PEN; a contact resistance (R_{CO}), representing the physical

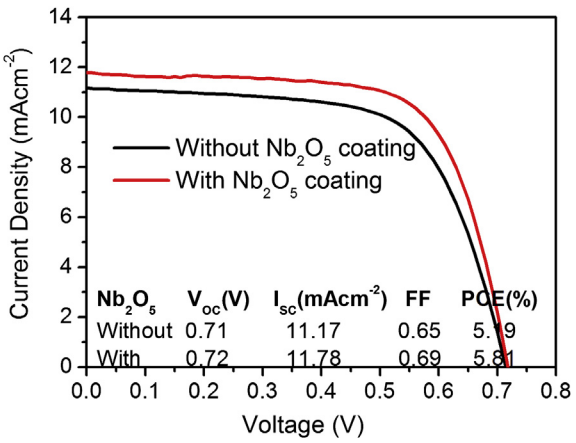

Fig. 7. *IV* curves of DSSCs composed of a plastic photoanode with and without Nb_2O_5-treated ITO PEN film and Pt-sputtered counter electrode.

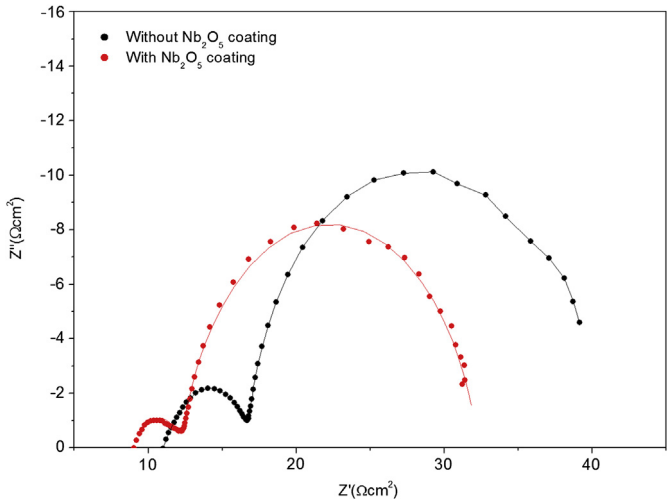

Fig. 8. EIS measured at open circuit condition under 1 sun illumination for DSSCs made from plastic photoanode with and without Nb_2O_5-treated ITO PEN film. The solid dots are the experimental data and the solid lines are fitting curves.

contact of ITO PEN and dye/TiO_2 film; a parallel combination of charge loss on the TiO_2/tri-iodide interface (R_{CT}) and ITO PEN/TiO_2 interface (R_{TCO}); a charge transfer resistance on the Pt/tri-iodide interface (R_{Pt}); and a diffusion impedance for the iodide/tri-iodide diffusion. The experimental data was fitted by this model and is summarized in Table 1.

It is revealed in Table 1 that R_S decreased from 11.28 to 9.12 Ω cm^2 after Nb_2O_5 coating. This decrease is attributed to the reduction of sheet resistance in the Nb-doping ITO film, as discussed above. Since R_S is one of the major parts of the total internal resistances in a DSSC [29], the benefit of smaller R_S will be an improvement FF in the *IV* curve, which agrees well with our data, as shown in Fig. 5. Secondly, it is worth noting that R_{CO} and R_{Pt} usually overlap one another in high frequency regions, since they typically appear as a single arc in a Nyquist plot. Moreover, since R_{CO} is slight in a well-assembled DSSC, some reports [28] have even omitted its contribution. However, in a device made on a flat or flexible substrate, such as ITO PEN [30] or stainless steel sheet [31], the contact between substrate and dye/TiO_2 film becomes important and

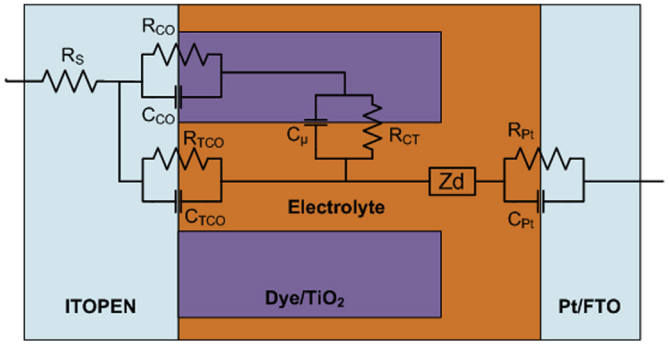

Fig. 9. Simplified transmission line model for the fitting of EIS data in this study. R_S is the series resistance of conductive substrate; R_{CO} and C_{CO} are the resistance and capacitance at substrate/TiO_2 contact; R_{TCO} and C_{TCO} are the charge transfer resistance and the corresponding double layer capacitance at exposed TCO/electrolyte surface; R_{CT} is the charge transfer resistance of the charge recombination at TiO_2/electrolyte interface; C_μ is the chemical capacitance of mesoporous TiO_2 film; Z_d is the Nernst diffusion impedance of redox species; and R_{Pt} and C_{Pt} are the charge transfer resistance and double layer capacitance at the counter electrode. Note that Z_d was omitted while fitting the curves due to the open circuit configuration, and all capacitance elements were replaced by constant phase elements (CPE) for better fitting accuracy.

Table 1
Fitting results of EIS data in Fig. 6.

Nb_2O_5 coating	R_S (Ω cm^2)	$R_{CO}+R_{Pt}$ (Ω cm^2)	$C_{CO}+C_{Pt}$ (μF)	R_{CT} (Ω cm^2)	C_μ (μF)
Without	11.28	5.32	15.22	24.17	149.8
With	9.12	3.13	41.07	20.03	185.6

should not be ignored. From Table 1, the sum of R_{Pt} and R_{CO} ($R_{PT}+R_{CO}$) shows a remarkable decrease from 5.32 to 3.13 Ω cm^2 after Nb_2O_5 coating. Since the counter electrodes were identical in both devices, the change in $R_{Pt}+R_{CO}$ after Nb_2O_5 coating was due to the change of R_{CO}, which means the contact resistance between the ITO PEN and dye/TiO_2 film decreased. As found in the FESEM topographical image, the Nb_2O_5-coated ITO surface creates many rugged nano-islands. Thus, it is a rational speculation that the decreased R_{CO} originates from the enhanced adherence of dye/TiO_2 and the Nb_2O_5-treated ITO surface, which reduces the ohmic loss in the interface and renders a better FF in the *IV* curve. By combining the decrease of R_S and R_{CO} in the DSSC with Nb_2O_5-coated ITO PEN, the FF consequently improves from 0.65 to 0.69.

The overall capacitance of ($C_{CO}+C_{Pt}$) was found to increase from 15.22 to 41.07 μF after Nb_2O_5 coating, and once again we attribute this increase to the contribution of C_{CO}, due to the fact that an identical platinized electrode was utilized in both tests. This finding indicates that the Nb_2O_5 modified substrate has more intense capacitive behavior at the interface because charge transfer through this interface has been suppressed, and so more charge is accumulated [30,32].

It also can be seen that the second arc in Fig. 8 shrank slightly after Nb_2O_5 coating. Though this arc represents the overall contribution from R_{CT} and R_{TCO}, we simplified the discussion by focusing on the effects of R_{CT} only, because the TiO_2 film is highly conductive under 1 sun illumination [26]. It is known that the more conductive the TiO_2 film, the easier the charge loss from the TiO_2/electrolyte interface; moreover, tri-iodide is in-situ formed by dye regeneration in open circuit conditions under illumination [33]. Therefore, the local concentration of tri-iodide in the vicinity of TiO_2/electrolyte interface will be higher than the bulk concentration. From Table 1, it can be seen that C_μ increases from 149.8 to 185.6 μF after Nb_2O_5 coating, indicating that the electron density of the plastic photoanode made with Nb_2O_5-coated ITO PEN is higher than that on an uncoated one. This finding is consistent with the observation that larger V_{OC} is found in an Nb_2O_5-coated cell as the conduction band edge position of the TiO_2 film shifts upward. On the other hand, the enhanced electron density also promoted charge recombination in the TiO_2/electrolye interface, and R_{CT} consequently decreased.

Through EIS analysis, we can conclude that the improvement of FF after it receives Nb_2O_5 nano-island coating is due to improved sheet resistance and better adherence, while the increase of I_{SC} and V_{OC} results from the suppression of the interfacial charge loss. Consequently, as an overall effect, PCE increased from 5.19% to 5.81%.

4. Conclusions

The PCE of plastic DSSC increased from 5.19% to 5.81%, which was achieved by coating Nb_2O_5 nano-islands on ITO PEN film using a low-temperature process. The improvement on PCE is attributed to the singular treatment between the ITO PEN substrate and dye/TiO_2 film, which was found to reduce the sheet resistance of ITO PEN, suppress interfacial charge loss and anchor the TiO_2 film more tightly. Since layer-to-layer adhesion strength is one of the key issues of this improvement on further application assessment, it is

therefore the future optimization of this treatment that is realized with niobium precursor concentration and spin-coating parameters, as well as quantitative adhesion strength measurement.

Acknowledgments

We are thankful for the financial support from the New Energy and Industrial Technology Development Organization (NEDO), Japan and the National Science Council, Taiwan (NSC 101-2218-E-007-010).

References

[1] B. O'Regan, M. Grätzel, Nature 353 (1991) 737.
[2] M.K. Nazeeruddin, A. Kay, R. Humphry-Baker, E. Müller, P. Liska, N. Vlachopoulos, M. Grätzel, J. Am. Chem. Soc. 115 (14) (1993) 6382.
[3] M. Grätzel, Inorg. Chem. 44 (2005) 6841.
[4] S. Ito, H. Matsui, K. Okada, S. Kusano, T. Kitamura, Y. Wada, S. Yanagida, Sol. Energy Mater. Sol. Cells 82 (2004) 421.
[5] A. Yella, H. Lee, H. Tsao, C. Yi, A. Chandiran, M.K. Nazeeruddin, E. Diau, C. Yeh, Science 334 (2011) 4.
[6] S. Ito, N.-L.C. Ha, G. Rothenberger, P. Liska, P. Comte, S.M. Zakeeruddin, P. Pechy, M.K. Nazeeruddin, M. Grätzel, Chem. Commun. (2006) 4004.
[7] M.G. Kang, N.G. Park, K.S. Ryu, S.H. Chang, K.J. Kim, Sol. Energy Mater. Sol. Cells 90 (2006) 574.
[8] T. Miyasaka, Y. Kijitori, J. Electrochem. Soc. 151 (2004) A1767.
[9] H.W. Chen, C.P. Liang, H.S. Huang, J.G. Chen, R. Vittal, C.Y. Lin, K.C.-W. Wu, K.C. Ho, Chem. Commun. 47 (2011) 8346.
[10] N.G. Park, K.M. Kim, M.G. Kang, K.S. Ryu, S.H. Chang, Y.J. Shin, Adv. Mater. 17 (2005) 2349.
[11] H. Lindstrom, A. Holmberg, E. Magnusson, S.-E. Lindquist, L. Malmqvist, A. Hagfeldt, Nano Lett. 1 (2001) 97.
[12] H. Lindstrom, E. Magnusson, A. Holmberg, S. Sodergren, S.E. Lindquist, A. Hagfeldt, Sol. Energy Mater. Sol. Cells 73 (2002) 91.
[13] T. Yamaguchi, N.T. Matsumoto, H. Arakawa, Chem. Commun. (2007) 4767.
[14] P.J. Cameron, L.M. Peter, S. Hore, J. Phys. Chem. B 109 (2005) 930.
[15] P.J. Cameron, L.M. Peter, J. Phys. Chem. B 107 (2003) 14394.
[16] S. Hore, R. Kern, Appl. Phys. Lett. 87 (2005) 263504.
[17] S. Lee, J.H. Noh, H.S. Han, D.K. Yim, D.H. Kim, J.K. Lee, J.Y. Kim, H.S. Jung, K.S. Hong, J. Phys. Chem. C 113 (2009) 6878.
[18] S.Q. Fan, B. Fang, H. Choi, S. Park, C. Kim, B.S. Jeong, J.J. Kim, J. Ko, Electrochim. Acta 55 (2010) 4642.
[19] J. Xia, N. Masaki, K. Jiang, S. Yanagida, Chem. Commun. (2007) 138.
[20] J. Xia, N. Masaki, K. Jiang, S. Yanagida, J. Photochem. Photobiol. A: Chem. 188 (2007) 120.
[21] Y. Kijitori, M. Ikegami, T. Miyasaka, Chem. Lett. 36 (2007) 190.
[22] T. Miyasaka, M. Ikegami, Y. Kijitori, J. Electrochem. Soc. 154 (2007) A455.
[23] N. Kikuchi, E. Kusano, E. Kishio, A. Kinbara, Vacuum 66 (2002) 365.
[24] K. Miettunen, J. Halme, P. Vahermaa, T. Saukkonen, M. Toivola, P. Lund, J. Electrochem. Soc. 156 (2009) B876.
[25] B. Yoo, K.-J. Kim, S.-Y. Bang, M.J. Ko, K. Kim, N.-G. Park, J. Electroanal. Chem. 638 (2010) 161.
[26] F. Fabregat-Santiago, J. Bisquert, G. Garcia-Belmonte, G. Boschloo, A. Hagfeldt, Sol. Energy Mater. Sol. Cells 87 (2005) 117.
[27] Q. Wang, S. Ito, M. Graetzel, F. Fabregat-Santiago, I. Mora-Sero, J. Bisquert, T. Bessho, H. Imai, J. Phys. Chem. B 110 (2006) 25210.
[28] F. Fabregat-Santiago, J. Bisquert, E. Palomares, L. Otero, D. Kuang, S.M. Zakeeruddin, M. Graetzel, J. Phys. Chem. C 111 (2007) 6550.
[29] L. Han, N. Koide, Y. Chiba, T. Mitate, Appl. Phys. Lett. 84 (2004) 2433.
[30] M. Manca, F. Malara, L. Martiradonna, L. DeMarco, R. Giannuzzi, R. Cingolani, G. Gigle, Thin Solid Films 518 (2010) 7147.
[31] Y. Jun, M.G. Kang, J. Electrochem. Soc. 154 (2007) B68.
[32] J. Shu, J. Liang, S. Peng, W. Xu, J. Pei, J. Chen, Solid State Sci. 11 (2009) 433.
[33] Q. Wang, J.-E. Moser, M. Graetzel, J. Phys. Chem. 109 (2005) 14945.